

# Gamma-oryzanol Stabilized Nanoliposomes for Enhanced Delivery of Hempseed Protein Hydrolysate: Physicochemical Characterization and Antioxidant Potential for Nutraceutical Applications

Muhammad Huzaifa Salem<sup>1</sup>, Akram Pezeshki<sup>1\*</sup>, Babak Ghanbarzade<sup>1,2</sup>, Hamed Hamishehkar<sup>3,4</sup>, Maryam Mohammadi<sup>5</sup>

## Abstract

**Background:** Hempseed protein hydrolysate (HPH) exhibits potent antioxidant activity but suffers from physicochemical instability and low bioavailability, limiting its pharmaceutical and nutraceutical applications. Sterol stabilizers can liposomal membrane integrity, yet comparative studies on their effects in HPH-loaded nanoliposomes remain limited.

**Objective:** To develop and characterize HPH-loaded nanoliposomes (HPH-NLs) stabilized with cholesterol (CHO), curcumin (CURC), and  $\gamma$ -oryzanol (GO), and to evaluate their physicochemical properties, encapsulation efficiency, structural characteristics, and antioxidant activity.

**Materials and Methods:** HPH was produced from hemp protein concentrate via pepsin-catalyzed enzymatic hydrolysis. Nanoliposomes were prepared using the thin-film hydration-sonication method. Formulations were characterized for particle size, polydispersity index (PDI), zeta potential, encapsulation efficiency (EE%), and morphology (SEM). Structural interactions were analyzed by Fourier transform infrared spectroscopy (FTIR) and differential scanning calorimetry (DSC). Antioxidant activity was monitored over 30-day storage.

**Results:** Enzymatic hydrolysis significantly enhanced HPH antioxidant activity compared to non-hydrolyzed protein (DPPH: 42.3% vs. 35.8%; ABTS<sup>•+</sup>: 41.1% vs. 39.1%). All formulations exhibited nanoscale dimensions (<110 nm). GO-stabilized nanoliposomes (GO-NL) demonstrated superior characteristics: smallest particle size ( $70 \pm 5$  nm), lowest PDI (0.183), highest EE% ( $92 \pm 2.1\%$ ), and greatest retention after 30 days (89.5%). FTIR confirmed HPH encapsulation through amide I/II bands. DSC revealed that GO eliminated the cooperative gel-to-liquid crystalline phase transition, indicating enhanced membrane stability. During storage, GO-NL maintained 90.5% of DPPH scavenging activity, significantly outperforming CURC-NL and CHO-NL ( $P \leq 0.05$ ).

**Conclusions:** GO functions as a dual-action stabilizer, simultaneously enhancing membrane integrity and providing antioxidant protection. GO-stabilized HPH nanoliposomes demonstrate enhanced physicochemical stability and antioxidant retention under in vitro storage conditions. These findings support further investigation of this system for potential nutraceutical applications, pending evaluation of release kinetics, gastrointestinal stability, and cellular uptake.

**Keywords:** Hempseed protein hydrolysate, Nanoliposomes, Gamma-oryzanol, Sterol stabilizers, Encapsulation efficiency, Antioxidant activity, Pharmaceutical delivery

## Introduction

The rising incidence of chronic non-communicable diseases—such as cardiovascular disorders, type 2 diabetes, and inflammatory conditions—has become a pressing global health concern. According to the World Health Organization, these diseases are expected to account for more than 30% of worldwide mortality. A central pathogenic mechanism underlying their progression is oxidative damage, driven by excessive free radical generation (1). While synthetic antioxidants and pharmaceutical interventions remain the mainstay of treatment, their long-term use is often associated with adverse effects such as toxicity, skin rashes, and metabolic

disturbances, prompting increased interest in natural, health-promoting alternatives (2).

Among natural bioactive compounds, protein-derived peptides have garnered considerable attention due to their diverse physiological benefits, including antioxidant, antihypertensive, and immunomodulatory activities (3,4). These bioactive peptides, typically consisting of 2–20 amino acid residues, are released from parent proteins through enzymatic hydrolysis and exhibit enhanced functional properties compared to intact proteins (5). Industrial hempseed (*Cannabis sativa* L.) has emerged as a particularly valuable source of such peptides, owing to its well-balanced amino acid profile,

Received 17 December 2025, Accepted 14 April 2026, Available online 30 April 2026

<sup>1</sup>Department of Food Science and Technology, Faculty of Agriculture, University of Tabriz, Tabriz, Iran. <sup>2</sup>Department of Food Engineering, Faculty of Engineering, Near East University, Cyprus, Mersin 10, Nicosia, Cyprus, Turkey. <sup>3</sup>Drug Applied Research Center, Tabriz University of Medical Sciences, Tabriz, Iran. <sup>4</sup>New Material and Green Chemistry Research Center, Khazar University, 41 Mehseti Street, Baku, AZ1096, Azerbaijan. <sup>5</sup>Department of Food Science and Engineering, Faculty of Agriculture, University of Kurdistan, Sanandaj, Iran

\*Corresponding Author: Akram Pezeshki, Tel: +989132311958, Akram.pezeshki@tabrizu.ac.ir



high digestibility, and hypoallergenic nature (6). Recent studies have shown that hempseed protein hydrolysates (HPH) exhibit strong antioxidant properties, effectively suppressing lipid peroxidation in food systems and demonstrating antiproliferative activity against cancer cell lines (2,7). Furthermore, hemp-derived peptides have shown intracellular antioxidant activity and potential chemoprotective properties, highlighting their therapeutic promise (7).

Despite these remarkable bioactivities, the practical application of HPH in pharmaceutical and nutraceutical formulations faces substantial challenges. These include physicochemical instability, susceptibility to thermal and oxidative degradation, low bioavailability, and undesirable sensory attributes such as bitterness (8). Encapsulation within lipid-based nanocarriers has proven to be an effective approach for addressing these limitations. Nanoliposomes, in particular, offer notable benefits, including biocompatibility, the ability to simultaneously incorporate both hydrophilic and hydrophobic agents, and protection of unstable bioactive compounds from environmental stressors (9). However, conventional liposomes often suffer from structural instability, aggregation, and premature leakage of encapsulated compounds (10). The incorporation of sterol-based stabilizers has been shown to enhance membrane integrity, with cholesterol (CHO) traditionally serving as the gold standard for bilayer reinforcement (4). Nevertheless, growing consumer demand for plant-based and CHO-free formulations has driven interest in alternative sterols, including curcumin (CURC) and  $\gamma$ -oryzanol (GO) (4,11).

GO, a unique mixture of ferulic acid esters of phytosterols and triterpene alcohols, is particularly noteworthy due to its dual functionality as both a membrane stabilizer and a potent antioxidant (11). Recent studies have demonstrated that GO can be effectively incorporated into liposomal formulations, where it not only reinforces bilayer structure but also serves as a natural prodrug, converting to ferulic acid in vivo and providing sustained antioxidant protection (12). Moreover, phytosterol-stabilized nanoliposomes have shown improved encapsulation efficiency, reduced particle size, and enhanced colloidal stability compared to conventional formulations (4,13).

While extensive research has explored nanoliposomal delivery of various bioactives, comparative investigations into the effects of different sterol stabilizers on HPH-loaded nanoliposomes remain limited. Therefore, this study aims to develop and characterize GO-stabilized nanoliposomes for enhanced delivery of HPH, with comprehensive evaluation of physicochemical properties, encapsulation efficiency, structural characteristics, and antioxidant activity. Among the formulations examined, GO-stabilized nanoliposomes demonstrated superior performance, achieving the smallest particle size (64.5 nm), highest encapsulation efficiency ( $95 \pm 2.1\%$ ), and enhanced antioxidant retention during storage,

positioning this system as a promising platform for pharmaceutical and nutraceutical applications.

## Materials and Methods

### Materials

Hemp seeds (*Cannabis sativa* L.) were procured from local markets in Isfahan, Iran. Pepsin (enzyme activity optimal at pH 7.4 and 40 °C) and Lipoid (phosphatidylcholine) were obtained from Tsuno Rice Chemicals (Japan). GO ( $\geq 98\%$  purity), CHO ( $\geq 99\%$  purity), CURC ( $\geq 95\%$  purity), and the free radical 2,2-diphenyl-1-picrylhydrazyl (DPPH) were purchased from Sigma-Aldrich (St. Louis, MO, USA). All other chemicals and reagents, including methanol, ethanol, hydrochloric acid, sodium hydroxide, potassium persulfate, ABTS (2,2'-azino-bis(3-ethylbenzothiazoline-6-sulfonic acid)), ferric chloride, potassium ferricyanide, trichloroacetic acid (TCA), and thiobarbituric acid (TBA), were of analytical grade and obtained from Merck Chemical Co. (Darmstadt, Germany). Double-distilled water was used throughout all experiments.

### Preparation of Hempseed Protein Concentrate

Hemp seeds were carefully cleaned, washed, and oven-dried at  $46 \pm 1$  °C. The dried seeds were subjected to cold pressing for oil removal, and the resulting defatted cake was milled into fine flour using a laboratory mill (Proctor Silex EI60) equipped with a 60-mesh sieve. The proximate composition of hempseed flour, including moisture, crude protein (nitrogen-to-protein conversion factor of 5.7), lipid, ash, and dietary fiber contents, was determined following standard AACC methods (44-15, 46-12, 30-20, 08-01, and 32-10, respectively). Total carbohydrate content was calculated by difference using equation [1]:

$$\% \text{ Carbohydrate} = 100 - (\% \text{ Moisture} + \% \text{ Lipid} + \% \text{ Protein} + \% \text{ Ash}) \quad [1]$$

Hempseed protein concentrate (HPC) was prepared according to the method of Živanović et al (14), with minor modifications. Defatted hempseed flour was dispersed in 0.8 M NaCl solution at a 1:10 (w/v) ratio, and the pH was adjusted to 9.0 using 2 N NaOH. The suspension was stirred continuously for 2 h at room temperature to ensure complete protein solubilization. Following centrifugation at 7000 rpm for 20 min at 4 °C, the supernatant was collected, and the pH was adjusted to 4.8 (the isoelectric point of hemp protein) using 2 N HCl to precipitate proteins. The precipitated protein pellet was recovered by centrifugation under the same conditions, washed, freeze-dried using a Christ freeze dryer (Germany), and stored at  $-18$  °C for subsequent analyses.

### Enzymatic Hydrolysis for Hempseed Protein Hydrolysate Production

HPH was prepared following the method of Sarabandi et al (15), with modifications. HPC was dissolved in phosphate

buffer (pH 7.4) at a concentration of 5% (w/v). Pepsin was added at an enzyme-to-substrate ratio of 2.5% (w/w), and the mixture was incubated at 40 °C under constant agitation (200 rpm) for 4 h to facilitate enzymatic hydrolysis. The enzymatic reaction was terminated by heating the solution at 95 °C for 15 min to inactivate the enzyme. Insoluble material was removed by centrifugation at 9000 rpm for 15 min at 4 °C, and the supernatant containing HPH was collected. The hydrolysate was freeze-dried and stored at -20 °C for further experimental use.

#### Amino Acid Profiling of Hempseed Protein Hydrolysate

The amino acid composition of HPH was analyzed using reverse-phase high-performance liquid chromatography (RP-HPLC), following the method described by Jiang et al (16). Protein samples were hydrolyzed with 6 N hydrochloric acid at 110 °C for 24 h under nitrogen atmosphere. Following hydrolysis, amino acids were derivatized using O-phthalaldehyde (OPA) and analyzed on a Young Lin Acme 9000 HPLC system (South Korea) equipped with a C18 column (4.6 × 150 mm, 3.1 μm particle size). Fluorescence detection was performed at 330 nm excitation and 480 nm emission wavelengths under isothermal conditions maintained at 35 °C. Amino acid identification and quantification were accomplished using standard amino acid mixtures. The essential amino acid index (EAAI) was calculated based on FAO/WHO reference patterns (2).

#### Evaluation of Antioxidant Activity of HPC and HPH

##### DPPH Radical Scavenging Activity

The DPPH radical scavenging activity was assessed according to the method of Akbarmehr et al. (17). Briefly, 1.5 mL of HPC or HPH solution (10 mg/mL) was mixed with an equal volume of 0.2 mM DPPH solution prepared in ethanol. The mixture was incubated in the dark at room temperature for 40 min to prevent photo-degradation. After incubation, samples were centrifuged at 7,000 rpm for 15 min, and the absorbance of the supernatant was measured at 517 nm using a UV-visible spectrophotometer (Ultraspec 2000, Pharmacia Biotech, England). The percentage inhibition was calculated using equation [2]:

$$\text{Inhibition (\%)} = [(A_{\text{blank}} - A_{\text{sample}}) / A_{\text{blank}}] \times 100 \quad [2]$$

where  $A_{\text{blank}}$  is the absorbance of the control (DPPH solution without sample) and  $A_{\text{sample}}$  is the absorbance of the sample.

##### ABTS<sup>+</sup> Radical Scavenging Activity

The ABTS<sup>+</sup> radical scavenging assay was performed following the procedure described by Sarabandi et al (18). ABTS<sup>+</sup> stock solution was prepared by mixing 7.45 mM ABTS with 2.45 mM potassium persulfate and allowing the mixture to react in the dark for 16 h at room

temperature. The working solution was diluted with 0.2 M phosphate-buffered saline (PBS, pH 7.4) to achieve an absorbance of  $0.70 \pm 0.02$  at 734 nm. Then, 30 μL of HPC or HPH solution (10 mg/mL) was added to 3 mL of ABTS<sup>+</sup> working solution, vortexed briefly, and incubated in the dark for 6 min. Absorbance was measured at 734 nm, and scavenging activity was calculated using equation 2.

##### Reducing Power Assay

The reducing power of HPC and HPH was evaluated following the method of Sarabandi et al (18). Briefly, 0.5 mL of sample solution (40 mg/mL) was mixed with 0.5 mL of 0.2 M phosphate buffer (pH 6.6) and 0.5 mL of 0.1% (w/v) potassium ferricyanide ( $K_3[Fe(CN)_6]$ ). The mixture was incubated at 55 °C for 20 min. The reaction was terminated by adding 0.5 mL of 10% (w/v) TCA, followed by centrifugation at 3000 rpm for 10 min. Then, 0.5 mL of the supernatant was mixed with 0.5 mL of distilled water and 0.2 mL of 0.1% (w/v) ferric chloride ( $FeCl_3$ ). After 10 min incubation at room temperature, absorbance was measured at 700 nm. Higher absorbance indicated greater reducing power.

##### Preparation of HPH-Loaded Nanoliposomes

HPH-loaded nanoliposomes (HPH-NLs) were prepared using the thin-film hydration technique combined with sonication, as described by Pezeshki et al (19) with modifications. For each formulation, 90 mg of lyophilized lecithin (Lipoid) was blended with 10 mg of the selected sterol stabilizer (CHO, CURC, or GO) and dissolved in 12 mL of absolute ethanol. The total lipid phase consisted of 90 mg lecithin + 10 mg sterol stabilizer, giving a lecithin:sterol weight ratio of 9:1. Based on the average molecular weight of lecithin (~775 g/mol) and each sterol (CHO 387 g/mol, CURC 368 g/mol, GO 603 g/mol). The sterol mol% relative to total lipid is ~31% for CHO, ~32% for CURC, and ~22% for GO. HPH was added at 7 mg per 11 mL final volume (0.636 mg/mL).

For preparing NLs, A few drops of Tween 80 were added to enhance solubilization. The mixture was transferred to a round-bottom flask and subjected to rotary evaporation (Heidolph, Germany) at 37 °C for 25 min to remove the organic solvent, forming a thin, uniform lipid film on the flask wall. For complete solvent removal, the flask was kept under vacuum overnight.

For hydration, 7 mg of freeze-dried HPH was dissolved in 1 mL of distilled water and added to the lipid film along with 10 mL of distilled water. Several glass beads were introduced to facilitate dispersion, and the mixture was gently stirred at room temperature for 30 min, producing multilamellar vesicles. To achieve nanoscale liposomes, the hydrated liposomal suspension was subjected to high-shear homogenization (Ultra-Turrax T25, IKA, Germany) at 20000 rpm for 20 min at a temperature above the lipid phase transition. The homogenized suspension was then cooled in an ice bath and processed using a probe

sonicator (Ultrasonic Processor, UP200H, Hielscher, Germany) at 80 Hz for 10 cycles of 1 min each, with 1 min rest intervals between cycles to prevent excessive heat-induced lipid degradation. This process ultimately yielded unilamellar nanoliposomes with significantly reduced particle dimensions. Blank liposomes (without HPH) were prepared following the same procedure.

#### Physicochemical Characterization of HPH-NLs

##### *Particle Size, Polydispersity Index, and Zeta Potential*

The mean particle size, polydispersity index (PDI), and zeta potential of HPH-NLs were determined using dynamic light scattering (DLS) on a Zetasizer Nano ZS system (Malvern Instruments, Worcestershire, UK) maintained at  $25 \pm 1$  °C. Prior to analysis, NL suspensions were diluted 1:100 with PBS (pH 7.4) to avoid multiple scattering effects and ensure optimal measurement conditions. All measurements were performed in triplicate, and results are reported as mean  $\pm$  standard deviation (19).

##### *Encapsulation Efficiency*

Encapsulation efficiency (EE%) was determined using ultrafiltration centrifugation. Briefly, 1 mL of HPH-NL suspension was mixed with 7 mL of 60% ethanol and transferred to Amicon Ultra-15 centrifugal filter units (10 kDa MWCO, Merck Millipore). Samples were centrifuged at 4000 rpm for 5 min. Ultrafiltration centrifugal filter units (10 kDa MWCO) were employed to separate free HPH from liposomes. The liposomes were subsequently disrupted with chloroform, and HPH content was quantified at 289 nm using a calibration curve ( $y = 0.1993x + 0.0536$ ,  $R^2 = 0.9958$ ). EE% was calculated using equation [3]:

$$EE\% = (\text{encapsulated HPH}/\text{initial HPH added}) \times 100 \quad [3]$$

##### *Encapsulation Stability During Storage*

The retention of HPH within NLs during storage was investigated according to Mohammadi et al (20). HPH-NL formulations were stored in sealed containers at 4°C for 28 days. At predetermined time intervals (days 7, 15, and 28), aliquots were withdrawn, and the amount of HPH remaining encapsulated was determined using the ultrafiltration method described in *Encapsulation Efficiency* section. The encapsulation stability (ES%) was calculated using equation [4]:

$$ES\% = (\text{Encapsulated HPH at day } t/\text{Initial encapsulated HPH}) \times 100 \quad [4]$$

##### *Scanning Electron Microscopy*

The morphological characteristics of HPH-NLs were examined using field emission scanning electron microscopy (FE-SEM, MIRA3, TESCAN, Czech Republic). One drop of diluted liposomal suspension was placed on a clean aluminum stub and allowed to air-dry at room temperature. Samples were sputter-coated

with a thin layer of gold under vacuum to render them conductive. Micrographs were captured at an accelerating voltage of 15 kV with various magnifications (13).

##### *Fourier Transform Infrared Spectroscopy*

Intermolecular interactions among nanoliposome components were examined using Fourier transform infrared spectroscopy (FTIR), following the procedure outlined by Akbarbaglu et al (17). Freeze-dried HPH, blank liposomes, and HPH-loaded NLs stabilized with different sterols were analyzed using an FTIR spectrophotometer (IRAffinity-1S, Shimadzu, Tokyo, Japan). Samples were finely ground with spectroscopic-grade potassium bromide (KBr) at a ratio of 1:100 and compressed into transparent pellets using a hydraulic press at 600 kg/cm<sup>2</sup>. Spectra were recorded in transmission mode over a wavenumber range of 4000–400 cm<sup>-1</sup> at a scanning speed of 4 mm/s with 32 scans per sample.

##### *Antioxidant Activity of HPH-NLs During Storage*

The antioxidant activity of HPH-NL formulations during 28 days of storage at 4 °C was evaluated using the DPPH radical scavenging assay as described in *DPPH Radical Scavenging Activity* section. Before analysis, NL samples were heated in a 100 °C water bath for 5 min to release encapsulated HPH before DPPH assay, as adapted from our previous work (13). Measurements were performed at days 0, 7, 15, and 28. Radical scavenging activity was calculated using equation [2], and results were expressed as percentage inhibition.

##### *Statistical Analysis*

Statistical analysis was performed using SPSS version 24. One-way analysis of variance (ANOVA) was applied to compare mean values among formulations (GO-NL, CURC-NL, CHO-NL) for each response variable (particle size, PDI, zeta potential, EE%, ES%, and antioxidant activity). When ANOVA indicated significant differences ( $P \leq 0.05$ ), post-hoc comparisons were conducted using Duncan's multiple range test. Degrees of freedom (df) were 2 for between-groups and 6 for within-groups (total  $n=9$  per formulation). All data are presented as mean  $\pm$  SD. Exact  $P$  values are reported in the text and figure legends where applicable (19).

## **Results**

### *Proximate Composition of Hempseed Flour*

The proximate composition of hempseed flour is presented in Table 1. Moisture content was  $9.8 \pm 0.02\%$ , ash  $5.67 \pm 0.03\%$ , crude fiber  $34.4 \pm 0.09\%$ , protein  $29.98 \pm 0.52\%$ , lipid  $10.12 \pm 0.03\%$ , and carbohydrate  $44.43 \pm 0.01\%$  (calculated by difference).

### *Amino Acid Composition of HPH*

RP-HPLC analysis of HPH (Table 2) revealed the presence of both essential and non-essential amino

**Table 1.** Proximate Composition of Hempseed Flour (% Dry Weight Basis)

| Parameter    | Value (% dry weight basis) |
|--------------|----------------------------|
| Moisture     | 9.8 ± 0.02                 |
| Ash          | 5.67 ± 0.03                |
| Crude fiber  | 34.4 ± 0.09                |
| Protein      | 29.98 ± 0.52               |
| Lipid        | 10.12 ± 0.03               |
| Carbohydrate | 44.43 ± 0.01               |

Values are expressed as mean ± standard deviation (n = 3). All determinations were performed on a dry weight basis. Protein content was calculated using a nitrogen-to-protein conversion factor of 5.7. Carbohydrate content was determined by difference: % Carbohydrate = 100 – (% Moisture + % Lipid + % Protein + % Ash).

**Table 2.** Amino Acid Composition of Hemp Seed Protein Hydrolysate Using Reverse-Phase High-Performance Liquid Chromatography

| Amino acid    | g/100 g |
|---------------|---------|
| Aspartic acid | 2.54    |
| Glutamic acid | 4.79    |
| Asparagine    | -       |
| Histidine     | 0.55    |
| Serine        | 1.03    |
| Glutamine     | -       |
| Arginine      | 2.7     |
| Citrulline    | -       |
| Glycine       | 0.97    |
| Threonine     | 0.75    |
| Alanine       | 0.96    |
| Tyrosine      | 0.83    |
| Methionine    | 0.25    |
| Valine        | 1.26    |
| Phenylalanine | 1.07    |
| Isoleucine    | 1.02    |
| Leucine       | 1.71    |
| Ornithine     | -       |
| Lysine        | 0.52    |
| Total         | 21.3    |

acids. Glutamic acid and aspartic acid showed the highest peak intensities. Essential amino acids including threonine, valine, methionine, lysine, and arginine were identified. Hydrophobic amino acids (valine, methionine, phenylalanine) eluted between 26–28 min.

EAAI was 0.92–0.95. Branched-chain amino acids (leucine, isoleucine, valine) comprised 17.8 of total amino acids. Arginine content was 10.7 %. Lysine was present at 3.7 g/100 g protein, methionine + cysteine at 2.8 g/100 g protein, and threonine at 3.5 g/100 g protein (Table 3).

### Antioxidant Activity of HPC and HPH

The antioxidant activities of HPC and its hydrolysate (HPH) are summarized in Table 4. HPH showed higher values in all assays compared to HPC. DPPH radical scavenging increased from 35.8 % (HPC) to 42.3% (HPH); ABTS<sup>+</sup> scavenging from 39.1 % to 42.3%; reducing power

**Table 3.** Amino acid profile of HPH Compared to FAO/WHO Reference

| Amino acid                 | HPH (g/100 g protein) | FAO/WHO adult requirement (g/100 g protein) |
|----------------------------|-----------------------|---|
| Threonine                  | 3.5                   | 2.3   |
| Lysine                     | 3.7                   | 4.5   |
| Branched chain amino acids | 17.8                  | 15  |
| Methionine + cysteine      | 2.8                   | 2.2   |
| Arginine                   | 10.7                  | -   |

Values represent the range from triplicate measurements. Amino acid analysis was performed by RP-HPLC following hydrolysis with 6 N HCl at 110°C for 24 h. FAO/WHO reference values are based on the 2021 protein quality assessment guidelines for adults. Branched-chain amino acids (BCAAs) include leucine, isoleucine, and valine. Methionine + cysteine are reported as sulfur-containing amino acids. (\*-) indicates no established requirement for non-essential amino acids.

**Table 4.** Antioxidant activities of HPC and HPH

| Sample | DPPH (%) | ABTS <sup>+</sup> (%) | Reducing power (Fe <sup>3+</sup> ) | Total antioxidant activity |
|--------|----------|-----------------------|------------------------------------|----------------------------|
| HPC    | 35.8     | 39.1                  | 0.93                               | 1.12                       |
| HPH    | 42.3     | 41.1                  | 2.15                               | 2.02                       |

Values are means of triplicate determinations (n = 3). DPPH radical scavenging was measured at 517 nm after 40 min incubation. ABTS<sup>+</sup> scavenging was measured at 734 nm after 6 min incubation. Reducing power was determined by conversion of Fe<sup>3+</sup> to Fe<sup>2+</sup>, measured at 700 nm; higher absorbance indicates greater reducing power. Total antioxidant activity was measured at 695 nm. HPC: hemp protein concentrate; HPH: hemp protein hydrolysate.

(Fe<sup>3+</sup>) from 0.93 to 2.15; and total antioxidant activity from 1.12 to 2.02.

### Characterization of HPH-Loaded Nanoliposomes

#### Particle Size, Polydispersity Index, and Zeta Potential

The particle size, PDI, and zeta potential of HPH-NLs stabilized with different stabilizers are shown in Table 5 and Figure 1. All formulations had mean diameters below 110 nm. GO-NL exhibited the smallest size (70 ± 5 nm) and lowest PDI (0.18). CHO-NL had a size of 105 ± 5 nm (PDI 0.3), and CURC-NL had 95 ± 5 nm (PDI 0.2). Zeta potential values were -14.2 mV (GO-NL), -21.3 mV (CURC-NL), and -10.3 mV (CHO-NL).

**Table 5.** Particle Size, Polydispersity Index, and Zeta Potential of HPH-NLs

| Stabilizer | Average diameter (nm) | PDI                      | Zeta potential (mV)    |
|------------|-----------------------|--------------------------|------------------------|
| GO-NL      | 70 ± 5 <sup>a</sup>   | 0.18 ± 0.03 <sup>a</sup> | -14.2 ± 1 <sup>b</sup> |
| CURC-NL    | 95 ± 5 <sup>a</sup>   | 0.2 ± 0.02 <sup>a</sup>  | -21.3 ± 2 <sup>a</sup> |
| CHO-NL     | 105 ± 5 <sup>a</sup>  | 0.3 ± 0.03 <sup>a</sup>  | -10.3 ± 2 <sup>c</sup> |

Values are expressed as mean ± standard deviation (n = 3). Different superscript letters within the same column indicate significant differences ( $P \leq 0.05$ ) as determined by Duncan's multiple range test. Particle size, polydispersity index (PDI), and zeta potential were measured by dynamic light scattering (DLS) at 25 ± 1°C after 1:100 dilution with phosphate-buffered saline (pH 7.4). CHO-NL: cholesterol-stabilized nanoliposomes; CURC-NL: Curcumin-stabilized nanoliposomes; GO-NL:  $\gamma$ -oryzanol-stabilized nanoliposomes; PDI, polydispersity index.

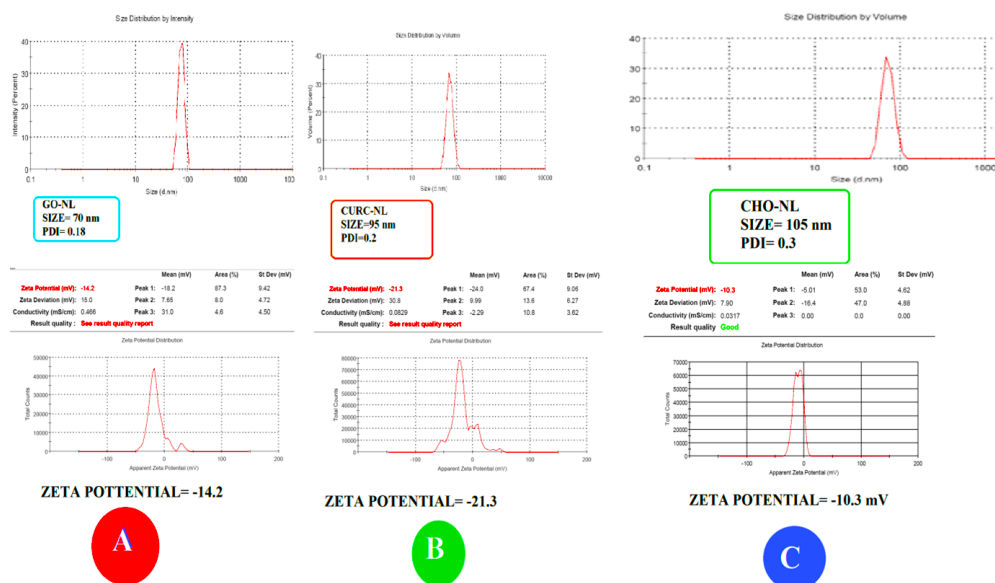


**Figure 1.** Particle Size Distribution, Polydispersity Index (PDI), and Zeta Potential Diagrams of Hempseed Protein Hydrolysate-Loaded Nanoliposomes (HPH-NLs) With Different Stabilizers: (A) Gamma-oryzanol (GO-NL), (B) Curcumin (CURC-NL), and (C) Cholesterol (CHO-NL).

### Morphology (SEM)

SEM images (Figure 2) showed spherical particles for all formulations. GO-NL displayed smooth surfaces and minimal aggregation. CHO-NL appeared uniform and well-dispersed. CURC-NL showed slightly irregular shapes and moderate aggregation. No significant morphological changes were observed after 30 days of storage at 4 °C.

### FTIR Analysis

FTIR spectra of HPH-NL (Figure 3) showed characteristic phospholipid bands: carbonyl ester C=O stretching at  $\sim 1740\text{ cm}^{-1}$  and phosphate P=O stretching at  $\sim 1240\text{ cm}^{-1}$ . In HPH-loaded formulation, amide I ( $\sim 1650\text{ cm}^{-1}$ ) and amide II ( $\sim 1550\text{ cm}^{-1}$ ) bands appeared, confirming peptide encapsulation. Shifts in these bands were observed compared to blank liposomes. In GO-NL, aromatic C–H stretching ( $815\text{--}672\text{ cm}^{-1}$ ) decreased in intensity, and bending vibrations of C=C–H and C–H ( $672\text{--}601\text{ cm}^{-1}$ )

were prominent. N–H bending ( $1650\text{--}1580\text{ cm}^{-1}$ ) shifted and intensified. C–H stretching of alkane chains ( $2850\text{--}3000\text{ cm}^{-1}$ ) was present in GO-NL and HPH-GO-NL but absent in free HPH.

### Differential Scanning Calorimetry

DSC thermogram (Figure 4) showed that GO-stabilized formulations suppressed the sharp gel-to-liquid crystalline phase transition of phospholipids. CHO-NL exhibited a broad, low-energy endotherm. CURC-NL showed a broadened endotherm with a slightly higher transition temperature. GO-NL displayed a sharper endotherm at approximately  $52\text{ }^{\circ}\text{C}$  with the smallest enthalpy change.

### Encapsulation Efficiency and Encapsulation Stability

EE% was highest for GO-NL ( $92 \pm 2\%$ ), followed by CURC-NL ( $87 \pm 1.5\%$ ) and CHO-NL ( $81 \pm 2\%$ ). After 30 days storage at  $4^{\circ}\text{C}$ , the retained encapsulation (ES%) was

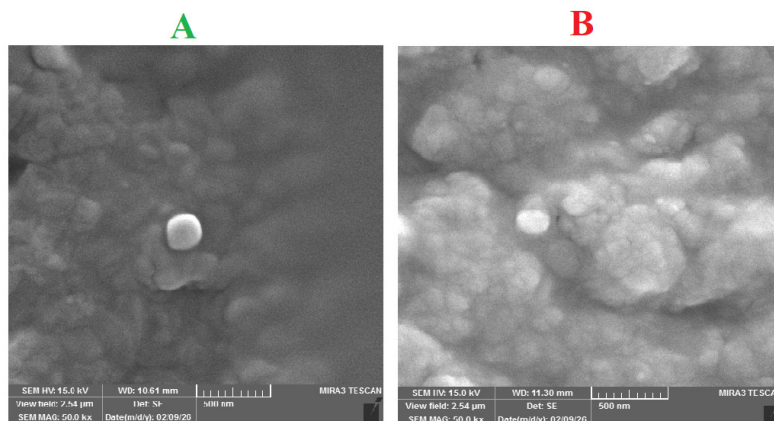


**Figure 2.** Scanning Electron Microscopy Images of Hempseed Protein Hydrolysate-Loaded Nanoliposomes With Different Stabilizers: (A) cholesterol (CHO-NL), (B) Curcumin (CURC-NL), and (C) Gamma-oryzanol (GO-NL). Magnification:  $\times 50\,000$ ; scale bar: 200 nm.

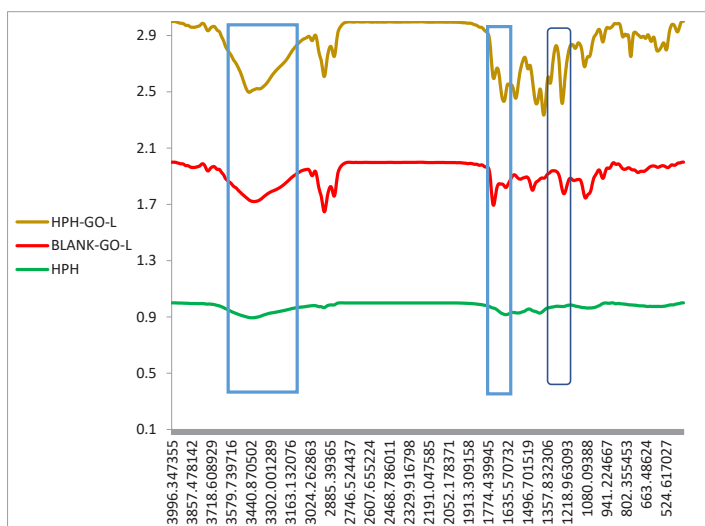


Figure 3. FTIR spectra of hempseed protein hydrolysate-loaded nanoliposome (HPH-NL) with GO stabilizer and Blank-NL.

89.5% (GO-NL), 83.8% (CURC-NL), and 77% (CHO-NL) of initial values.

**Antioxidant Activity During Storage**

DPPH radical scavenging activity (Figure 5) followed a similar trend. Initial activities were 48.3% (GO-NL), 35.9% (CURC-NL), and 29.1% (CHO-NL). After 30 days, activities were 43.1% (GO-NL, 90.5% retention), 32.1% (CURC-NL, 89.3% retention), and 21.7% (CHO-NL, 52.7% retention). Phenolic content and antioxidant activity showed strong correlation.

**Discussion**

Analysis of the proximate composition of hempseed flour confirmed its value as a nutrient-dense material, providing high levels of protein (29.98%) and dietary fiber (34.4%), in agreement with previous findings (2,6). The protein

content is comparable to other oilseeds, supporting its use as a sustainable plant protein source for nutraceutical applications.

The amino acid profile of HPH revealed a well-balanced essential amino acid composition, with an EAAI (0.92–0.95) exceeding that of soy and pea proteins (2). The elevated levels of branched-chain amino acids (15–20%) are particularly important for stimulating muscle protein synthesis, while the high arginine content (10–12%) may support cardiovascular health through nitric oxide-mediated vasodilation (6,7). The presence of hydrophobic amino acids, which eluted later in RP-HPLC, is advantageous for antioxidant activity, as these residues facilitate interactions with lipid radicals (22).

Enzymatic hydrolysis with pepsin significantly enhanced the antioxidant activity of HPH compared to HPC across multiple assays (23). This improvement

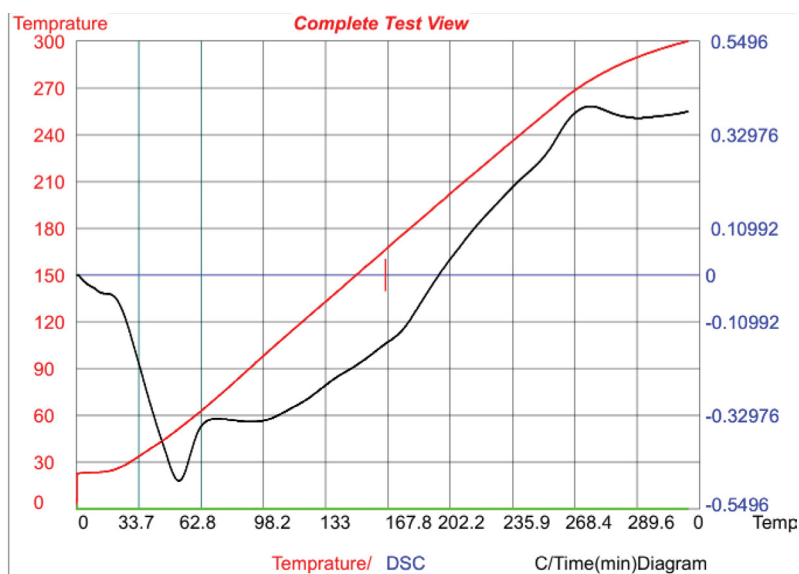
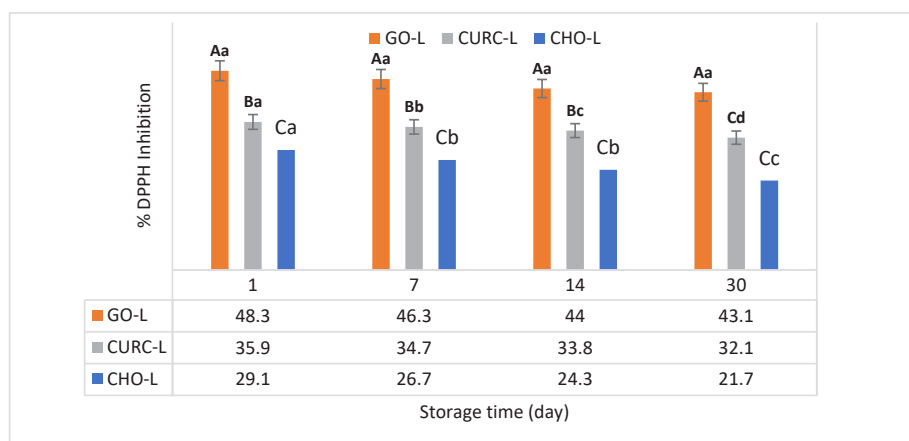


Figure 4. DSC thermogram of Hempseed Protein Hydrolysate- Loaded Nanoliposome With GO Stabilizer.



**Figure 4.** DPPH Radical Scavenging Activity of Hempseed Protein Hydrolysate-Loaded Nanoliposomes (HPH-NLs) With Different Stabilizers: Cholesterol (CHO-NL), Curcumin (CURC-NL), and Gamma-oryzanol (GO-NL).

is attributed to the release of low-molecular-weight peptides during hydrolysis, which exposes hidden amino acid residues with radical-quenching capacity (23). The increase in reducing power (from 0.93 to 2.15) indicates that HPH peptides can act as electron donors, converting  $Fe^{3+}$  to  $Fe^{2+}$ . These findings align with previous studies on protein hydrolysates from quinoa and flaxseed (3,15). The presence of tyrosine at C-terminal positions, known to inhibit lipid oxidation, may further contribute to the observed activity (22).

The physicochemical characteristics of HPH-NLs were strongly influenced by the type of stabilizer. GO-NL exhibited the smallest particle size (70 nm) and lowest PDI (0.18), indicating a narrow size distribution suitable for positioning this system as a promising platform for further evaluation in food and nutraceutical matrices (19). This can be explained by the amphiphilic nature of GO, whose ferulic acid moiety provides steric stabilization and hydrogen-bonding interactions, enhancing vesicle curvature and preventing aggregation (11,14). In contrast, CURC-NL formed larger vesicles (105 nm) with higher PDI, likely due to the ketone groups of CURC disrupting uniform bilayer packing and promoting hydrophobic-driven fusion (4,13). CHO-stabilized liposomes exhibited intermediate properties, consistent with CHO's role in condensing lipid bilayers without the incorporation of bulky side chains (19).

The zeta potential values reflect surface charge and colloidal stability. CURC-NL exhibited the most negative zeta potential ( $-21.3$  mV), which theoretically favors electrostatic repulsion. However, the larger particle size and irregular morphology observed in SEM suggest that steric effects may dominate over electrostatic stabilization in this formulation. GO-NL, despite a lower absolute zeta potential ( $-14.2$  mV), demonstrated superior colloidal stability due to the steric barrier created by its ferulic acid moiety (13).

SEM images confirmed the spherical morphology and nanoscale dimensions of all formulations, with GO-NL

showing the smoothest surfaces and least aggregation. This morphological uniformity is critical for predictable release kinetics and bioavailability (9). The absence of significant changes after 30-day storage indicates good physical stability, particularly for GO-NL.

FTIR analysis provided molecular-level evidence of successful HPH encapsulation. The appearance of amide I and II bands in loaded formulations, absent in blank liposomes, confirmed peptide incorporation. Shifts in these bands suggest hydrogen bonding between HPH peptides and the lipid bilayer (17). In GO-NL, the broadening of amide bands and changes in C-H stretching vibrations indicate strong interactions between GO's phenolic hydroxyl groups and phospholipid headgroups, reinforcing membrane integrity (13,24). These interactions are consistent with previous reports on ferulic acid-sterol conjugates (25).

DSC thermograms demonstrated that all stabilizers influenced the phase behavior of the lipid bilayer. The attenuation of the sharp gel-to-liquid crystalline transition suggests enhanced membrane rigidity and increased packing density (26). CHO's ability to eliminate cooperative phase transitions is well-documented, creating a liquid-ordered phase that stabilizes liposomes (27). CURC exhibited distinct behavior, with a slightly higher transition temperature suggesting partial ordering (28). GO produced the most pronounced effect, with a sharp endotherm at  $52$  °C and minimal enthalpy change, reflecting its dual anchoring mechanism: the sterol tail inserts into the hydrophobic core while the ferulic acid head hydrogen-bonds at the interface (24,29). This unique behavior enhances thermal stability and resistance to phase transition, which is advantageous for formulations intended for thermal processing.

Encapsulation efficiency was highest for GO-NL (92%), followed by CURC-NL (87%) and CHO-NL (81%). The superior EE% of GO-NL can be attributed to its amorphous bilayer structure, which creates greater free volume for peptide accommodation, and the additional

peptide-binding sites provided by the ferulic acid moiety through hydrogen bonding and  $\pi$ - $\pi$  stacking with aromatic amino acids (22). The lower EE% of CHO-NL may result from imperfect bilayer packing, as suggested by SEM and particle size data. The encapsulation stability data demonstrate that GO-NL retains HPH most effectively over 30 days (89.5% retention), indicating that GO not only facilitates initial loading but also prevents leakage during storage. This is consistent with the DSC findings, which showed that GO eliminates phase transition-associated defects that could cause premature release (26).

Comparing the DPPH radical scavenging activity of free HPH (non-encapsulated) versus encapsulated HPH in GO-NL during 30 days of storage at 4°C, showed lost 68.5% of its initial antioxidant activity after 30 days (from 42.3% to 13.3% inhibition). retained 90.5% of encapsulated HPH in GO-NL activity (from 48.3% to 43.1% inhibition). In addition, the protective effect (encapsulated vs. free) was statistically significant ( $P < 0.001$ ) from day 7 onward.

The retention of antioxidant activity during storage followed the order GO-NL > CURC-NL > CHO-NL. The superior performance of GO-NL is attributable to GO's intrinsic antioxidant properties. Its ferulic acid moiety, positioned at the membrane interface, can scavenge radicals and terminate lipid peroxidation chain reactions (24). Moreover, hydrogen bonding between ferulic acid and phospholipid headgroups reinforces bilayer cohesion, reducing permeability and oxidative degradation (13). The strong correlation between phenolic content and antioxidant activity ( $R^2 > 0.95$ ) confirms that phenolics are the primary contributors to radical scavenging in these formulations.

The rapid decline in antioxidant activity of CHO-NL may reflect diminished synergy among phenolic compounds during storage, as observed in other nanoencapsulation systems (4,30). CURC-stabilized liposomes showed intermediate retention, consistent with its membrane-stabilizing role (4).

The novelty of the present study lies in three specific aspects. First, while GO has been incorporated into liposomes with synthetic antioxidants or vitamins (12,13), its combination with a pepsin-generated HPH has not been previously reported. Second, compared to the closely related work on Spirulina protein hydrolysate-loaded GO liposomes (which used alcalase and flavourzyme), our pepsin-only protocol produced a distinct peptide profile enriched in hydrophobic amino acids (valine, methionine, phenylalanine) and arginine (10.7%), which are known to enhance membrane interactions and radical scavenging. Third, while Mohammadi et al (4) reviewed phytosterol-stabilized nanocarriers, the present study provides experimental evidence that GO eliminates the gel-to-liquid crystalline phase transition (DSC data), a finding not previously demonstrated for HPH-loaded systems. This combination of pepsin-derived HPH with GO-stabilized nanoliposomes, supported by comprehensive

FTIR and DSC mechanistic data, represents a distinct contribution to the field.

### Limitations of the Study

The authors acknowledge several limitations. First, the study was conducted entirely under in vitro conditions; no in vivo experiments (animal or human) were performed, and therefore bioavailability, biodistribution, and therapeutic efficacy remain unknown. Second, release kinetics were not evaluated; we did not perform dialysis-based release studies or simulated gastrointestinal digestion. Third, cytotoxicity and cellular uptake studies (e.g., on Caco-2 or other intestinal models) were not conducted. Fourth, the storage study was limited to 30 days at 4°C; long-term stability at ambient or accelerated conditions was not assessed. Fifth, the HPH used was a crude hydrolysate; further fractionation and identification of individual peptide sequences could provide mechanistic insights. These limitations do not invalidate the findings but highlight the need for future research before any pharmaceutical application can be considered.

### Conclusions

GO acts as a multifunctional stabilizer that enhances particle size distribution, encapsulation efficiency, and thermal stability of HPH-loaded nanoliposomes, while also protecting against oxidative degradation during storage. However, the current study is limited to in vitro physicochemical and antioxidant characterization. No conclusions can yet be drawn regarding release kinetics, gastrointestinal stability, cytotoxicity, or in vivo efficacy. Future studies should evaluate these parameters, including simulated digestion, intestinal permeability, and cellular antioxidant activity, before any pharmaceutical application can be considered.

### Authors' Contribution

**Conceptualization:** Babak Ghanbarzadeh, Hamed Hamishehkar.  
**Data curation:** Hamed Hamishehkar, Maryam Mohammadi.  
**Formal analysis:** Muhammad Huzaifa Salem, Maryam Mohammadi.  
**Investigation:** Muhammad Huzaifa Salem.  
**Project administration:** Babak Ghanbarzadeh.  
**Supervision:** Akram Pezeshki, Babak Ghanbarzadeh.  
**Validation:** Hamed Hamishehkar.  
**Writing—original draft:** Muhammad Huzaifa Salem.  
**Writing—review & editing:** Akram Pezeshki.

### Conflict of Interests

None declared.

### Data availability Statement

Data will be made available on request from the corresponding author.

### Ethical Issues

The authors declare that no experiments were conducted on animals and humans in this research.

### Financial Support

This paper is derived from the PHD thesis of Muhammad Huzaifa, conducted at the Faculty of Agriculture, University of Tabriz, Tabriz, Iran, under proposal number 13/475772/1 dated November 13, 2023.

This research was co-supported by the University of Tabriz and the Drug Applied Research Center, Tabriz University of Medical Sciences.

## References

- World Health Organization. Noncommunicable diseases progress monitor 2025. World Health Organization; 2025.
- Santos-Sánchez G, Álvarez-López AI, Ponce-Espana E, et al. Hempseed (*Cannabis sativa*) protein hydrolysates: A valuable source of bioactive peptides with pleiotropic health-promoting effects. *Trends Food Sci Technol*. 2022;127:303-18.
- Daliri H, Ahmadi R, Pezeshki A, et al. Quinoa bioactive protein hydrolysate produced by pancreatin enzyme-functional and antioxidant properties. *LWT*. 2021;150:111853. doi:10.1016/j.lwt.2021.111853
- Mohammadi M, Jafari SM, Hamishehkar H, Ghanbarzadeh B. Phytosterols as the core or stabilizing agent in different nanocarriers. *Trends Food Sci Technol*. 2020;101:73-88.
- Ahaninjan M, Peighambari SH, Azadmard-Damirchi S. From plant to nanomaterial: Physicochemical and functional characterization of nanochitosomes loaded with antioxidant peptide fractions from oleaster-seed protein. *J Agric Food Res*. 2025;20:101771. doi:10.1016/j.jagr.2025.101771
- Barretto R, Qi G, Xiao R, et al. Hempseed protein is a potential alternative source for plant protein-based adhesives. *Int J Adhes Adhes*. 2024;133:103740. doi:10.1016/j.jadhadh.2024.103740
- Montserrat-de la Paz S, Carrillo-Berdasco G, Rivero-Pino F, Villanueva-Lazo A, Millan-Linares MC. Hemp Protein Hydrolysates Modulate Inflammation-Related Genes in Microglial Cells. *Biology (Basel)*. 2022;12(1):49. doi:10.3390/biology12010049
- Liu W, Hou Y, Jin Y, Wang Y, Xu X, Han J. Research progress on liposomes: Application in food, digestion behavior and absorption mechanism. *Trends Food Sci Technol*. 2020;104:177-89.
- Prabhakar P, Tripathy S, Verma DK, et al. Trends and advances in liposome formulation technology with an emphasis on ensuring safety and quality in food and drug applications. *Food Bioscience*. 2025;69:106913.
- Hashemi FS, Farzadnia F, Aghajani A, Ahmadzadeh Nobari Azar F, Pezeshki A. Conjugated linoleic acid loaded nanostructured lipid carrier as a potential antioxidant nanocarrier for food applications. *Food Sci Nutr*. 2020;8(8):4185-95.
- Pansiri S, Duangsrisai S. Health properties of  $\gamma$ -oryzanol and its applications: A review. *J Funct Food*. 2025;134:107064.
- Yadav P, Sankar J, Mora C, et al. Nanoencapsulated  $\gamma$ -oryzanol enhances fibroblast proliferation, migration, and reduces oxidative stress in H<sub>2</sub>O<sub>2</sub>-induced cellular aging model. *J Funct Food*. 2026;136:107130.
- Amiri S, Ghanbarzadeh B, Hamishehkar H, Hosein M, Babazadeh A, Adun P. Vitamin E loaded nanoliposomes: effects of gamma-oryzanol, polyethylene glycol and lauric acid on physicochemical properties. *Colloid and Interface Science Communications*. 2018;26:1-6.
- Živanović I, Vaštag Z, Popović S, Popović L, Peričin D. Hydrolysis of hullless pumpkin oil cake protein isolate by pepsin. *International Journal of Biological, Biomolecular, Agricultural, Food and Biotechnological Engineering*. 2011;5(3):94-98.
- Sarabandi K, Jafari SM, Mohammadi M, Akbarbaglu Z, Pezeshki A, Heshmati MK. Production of reconstitutable nanoliposomes loaded with flaxseed protein hydrolysates: Stability and characterization. *Food Hydrocolloids*. 2019;96:442-50. doi:10.1016/j.foodhyd.2019.05.047
- Jiang Y, Sun J, Chandrapala J, et al. Recent progress of food-derived bioactive peptides: Extraction, purification, function, and encapsulation. *Food Front*. 2024;5(3):1240-64.
- Akbarmehr A, Peighambari SH, Ghanbarzadeh B, Sarabandi K. Physicochemical, antioxidant, antimicrobial, and in vitro cytotoxic activities of corn pollen protein hydrolysates obtained by different peptidases. *Food Sci Nutr*. 2023;11(5):2403-2417. doi:10.1002/fsn3.3252
- Sarabandi K, Karami Z, Akbarbaglu Z, Duangmal K, Jafari SM. Spray-drying stabilization of oleaster-seed bioactive peptides within biopolymers: Pan-bread formulation and bitterness-masking. *Food Bioscience*. 2024;58:103837.
- Pezeshki A, Ghanbarzadeh B, Hamishehkar H, Moghadam M, Babazadeh A. Vitamin A palmitate-bearing nanoliposomes: Preparation and characterization. *Food Bioscience*. 2016;13:49-55.
- Mohammadi M, Ghanbarzadeh B, Hamishehkar H. Formulation of nanoliposomal vitamin D<sub>3</sub> for potential application in beverage fortification. *Adv Pharm Bull*. 2014;4(Suppl 2):569-575. doi:10.5681/apb.2014.084
- Fatahi H, Claverie J, Poncet S. Thermal characterization of phase change materials by differential scanning calorimetry: a review. *Appl Sci*. 2022;12(23):12019. doi:10.3390/app122312019
- Shi C, Liu M, Zhao H, Lv Z, Liang L, Zhang B. A novel insight into screening for antioxidant peptides from hazelnut protein: Based on the properties of amino acid residues. *Antioxidants*. 2022;11(1):127.
- Peng X, Kong B, Xia X, Liu Q. Reducing and radical-scavenging activities of whey protein hydrolysates prepared with Alcalase. *International Dairy Journal*. 2010;20(5):360-5.
- Phothi T, Tunsophon S, Tiyaboonchai W, Khongsombat O. Effects of curcumin and  $\gamma$ -oryzanol solid dispersion on the brain of middle-aged rats. *Biomed Rep*. 2022;17(1):59. doi:10.3892/br.2022.1542
- Juricic H, Cuccioloni M, Bonfili L, et al. Biochemical, Biological, and clinical properties of  $\gamma$ -Oryzanol. *Antioxidants*. 2025;14(9):1099.
- Tai K, Rappolt M, Mao L, Gao Y, Yuan F. Stability and release performance of curcumin-loaded liposomes with varying content of hydrogenated phospholipids. *Food Chem*. 2020;326:126973. doi:10.1016/j.foodchem.2020.126973
- Krause MR, Regen SL. The structural role of cholesterol in cell membranes: from condensed bilayers to lipid rafts. *Accounts of Chemical Research*. 2014;47(12):3512-21.
- Patra A, Jha S, Murthy P, Manik SA, Sharone A. Isolation and characterization of stigmast-5-en-3 $\beta$ -ol (Curcumin) from the leaves of *Hygrophila spinosa* T. Anders. *Int J Pharma Sci Res*. 2010;1(2):95-100.
- Patel M, Naik S.  $\Gamma$ -oryzanol from rice bran oil: a review. *J Sci Ind Res*. 2004;63(7):569-78.
- Giannopoulos-Dimitriou A, Saiti A, Petrou A, Vizirianakis IS, Fatouros DG. Liposome stability and integrity. In: *Liposomes in drug delivery*. Elsevier; 2024. p. 89-121.

**Copyright** © 2026 The Author(s); This is an open-access article distributed under the terms of the Creative Commons Attribution License (<http://creativecommons.org/licenses/by/4.0>), which permits unrestricted use, distribution, and reproduction in any medium, provided the original work is properly cited.